NOTES AND CORRESPONDENCE

Design and Deployment of a Portable, Pencil-Beam, Pulsed, 3-cm Doppler Radar

JOSHUA WURMAN AND JERRY STRAKA

School of Meteorology, University of Oklahoma, Norman, Oklahoma

ERIK RASMUSSEN

National Severe Storms Laboratory, National Oceanic and Atmospheric Administration, Norman, Oklahoma

MITCH RANDALL

Atmospheric Technology Division, National Center for Atmospheric Research, Boulder, Colorado

ALLEN ZAHRAI

Operational Support Facility, National Weather Service, Norman, Oklahoma

28 March 1996 and 12 January 1997

ABSTRACT

A portable, pencil-beam, pulsed, Doppler, 3-cm wavelength radar has been constructed to study a wide variety of meteorological phenomena including tornadoes, severe storms, and boundary layer processes. The new radar, the Doppler on Wheels (DOW), has full scanning capability, a real-time display and archiving, and is mounted on a truck for easy portability and full mobility. This portability allows the radar to be brought to within a kilometer of rare meteorological phenomena. At this range, the pencil beam of the radar is very narrow, permitting significantly higher-resolution measurements (at 3-km range, 64 m × 64 m × 75 m) than are usually possible with stationary or airborne systems. The radar employs a new high-powered, PC-based, digital intermediate frequency (IF) data acquisition scheme called the PIRAQ.

The radar has successfully collected data in several tornadoes and tornadic storms and has been used to detect dust devils and other boundary layer structures. The sensitivity and mobility of the radar permits two-dimensional traveling vertical wind profiles to be obtained, extending the applicability of traditional one-dimensional profilers. Other applications are possible, including avian and entomological studies, pseudo-dual-Doppler, and rainfall estimation following and rapidly scanning storms in conjunction with mobile rain gauges.

1. Introduction and motivation

This paper documents the design and early deployment of a mobile Doppler radar. Many of the most interesting and important meteorological phenomena occur infrequently and/or very near the ground. These are difficult to measure with traditional stationary meteorological radars. Such phenomena include tornadoes (e.g., Bluestein and Golden 1993; Fujita 1978; Wakimoto et al. 1996), microburst outflows (Wakimoto and Bringi 1988), dust devils (Snow and McClelland 1990), waterspouts (Schwiesow 1981), landspouts (Wakimoto and Wilson 1989), and landfalling hurricanes (Wakimoto and Black 1994; Kaplan and Demaria 1995). Moreover, many interesting physical processes occur at subkilometer scales, but the ranges between the phenomena of interest and the stationary radars are almost always quite large. This results in finescale (subkilometer) structures being unresolvable due to beam spreading between stationary radars and the targets. Near-ground (<300 m AGL) structures are undetectable due to the masking of the transmitted beam by topography and obstructions, vertical beam spreading, and earth curvature. Finally, these phenomena frequently occur on timescales of seconds to minutes and thus are sampled poorly by typical surveillance radar scanning strategies. There is a need for finescale observations of these phenomena in order to better understand the mechanisms involved in their formation and maintenance (Kaplan and Damaria 1995; Brandes 1993; Bluestein et al. 1993; Bluestein and Golden 1993; Zrnic et al. 1985).

Corresponding author address: Dr. Joshua Wurman, School of Meteorology, University of Oklahoma, Norman, OK 73019.

2. Beam spreading and masking

Stationary radars are poorly suited for the study of many near-ground and finescale phenomena. Spreading causes even 1° radar beams to widen to 1 km at a range of 57 km. Atmospheric structures at smaller scales cannot be resolved at these ranges. Masking of the lower portion of radar beams by topography, vegetation, or structures can prevent measurements near the surface. This effect is highly variable depending on the local terrain and can be quite significant. Furthermore, earth curvature effects contribute to the difficulty of obtaining near-ground measurements, though this factor is usually smaller than that caused by beam spreading. Beam curvature due to atmospheric refractive gradients does not prevent finescale or near-ground measurements per se, but complicates analyses at great ranges by causing uncertainties in actual beam altitude (Doviak and Zrnic 1993). These effects can complicate observations of tornado structure and other phenomena (Burgess et al. 1993; Wilson 1986)

Infrequent meteorological events rarely occur in the immediate proximity of traditional stationary radars. To resolve structures on a scale of 100 m, or structures within 100 m of the ground, which is the resolution scale required in order to resolve tornadic phenomena, an object must be within 5.7 km of a 1° beam radar system. Thus, such a radar is surrounded by a 100-km^2 region in which 100-m structures can be resolved. A typical WSR-88D radar surveys an area of roughly 125 000 km^2 (the area within a 200-km radius of the radar). Thus, finescale and near-ground data (<100 m) can be retrieved in less than 1/1000 of the survey region and, therefore, only 1/1000 of randomly distributed small-scale weather phenomena (Fig. 1a). Approximately 1000 tornadoes occur annually in the United States. If these are evenly distributed over the 10^7-km^2 national area, then only one tornado is expected per 100 km^2 per 100 yr—requiring a very patient radar operator. Even in the tornado-prone regions of the Midwest, the mean time between such nearby tornado occurrences is roughly 10 yr.

This unfortunate situation is common even in research programs that deploy multiple radars for the purpose of retrieving multiple-Doppler windfield data. There is an obvious trade-off between the close spacing of radars (permitting higher-resolution measurements) and wide spacing of radars (permitting more storms to pass through a study area). Typically, multiple-Doppler studies have radars separated by 20–50 km (Ray et al. 1978; Miller 1978; Raymond and Blythe 1989; Harris and Fankhauser 1978; Lhermitte and Williams 1985) (Fig. 1b), although at least one experiment employed a dense network with 8–22-km baselines (Wurman 1991), which could have permitted multiple-Doppler data to be retrieved at the 100-m scale. Only rarely have infrequent phenomena occurred in the immediate proximity of even a single research radar (Bluestein and Golden 1993).

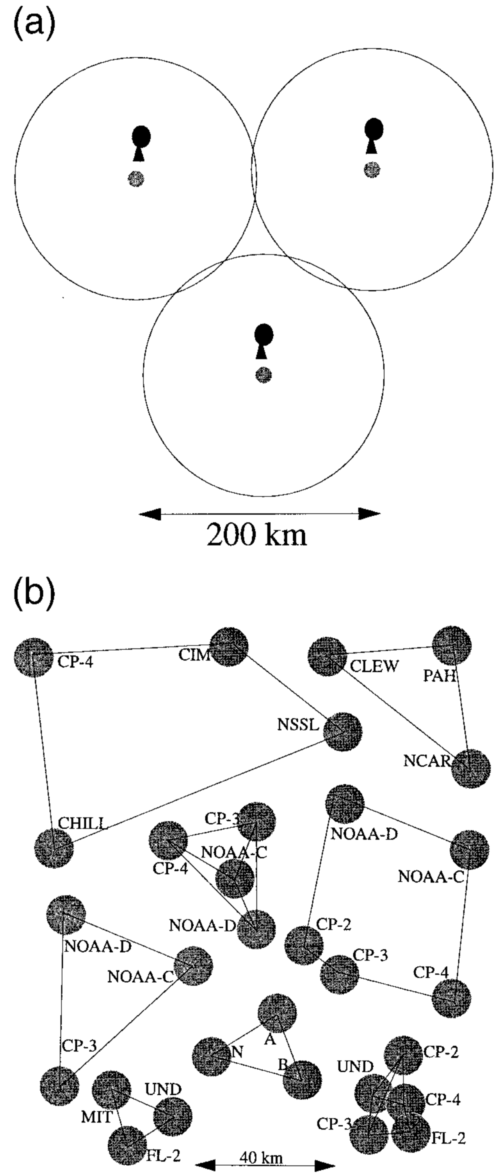

FIG. 1. (a) Typical distribution of WSR-88D operational radars with the 5.7-km-radius regions in which high-resolution, <100 m, data can be retrieved shaded. Shaded area is less than 0.001 of the total. (b) Various multiple-Doppler networks from various experiments. Clockwise from top left: Ray (1978), FACE, Harris and Fankhauser (1978), Wurman (1991), Lhermitte (1985), Wurman (1991), Miller (1978), in the center, Raymond and Blythe (1989). The shaded areas illustrate the 5.7-km-radius regions where high-resolution, <100 m, data can be retrieved. In only the Huntsville network, at the lower right, is high-resolution multiple-Doppler data even theoretically retrievable.

One notable example is the tornado that occurred 15–22 km from two NOAA radars (Wakimoto and Martiner 1992), resulting in beamwidths as low as 210 m.

Recently, airborne radars have demonstrated the value of their unequalled mobility, which has allowed them to collect data in rare weather, including tornadic storms and otherwise inaccessible locations, particularly at sea

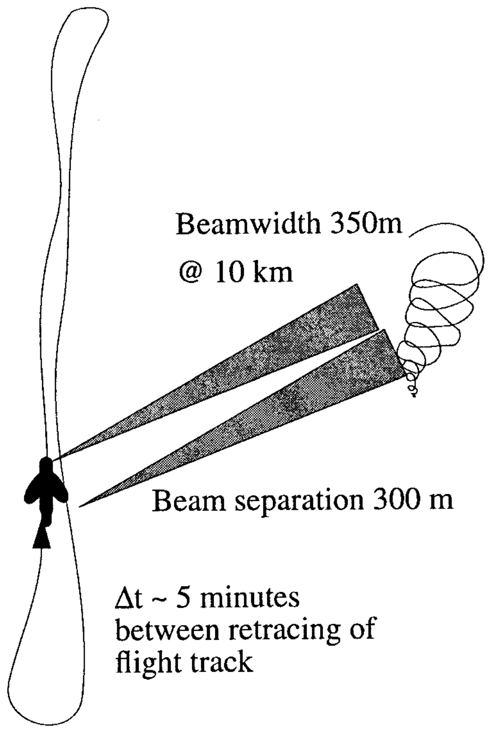

FIG. 2. Schematic of deployment of airborne radar near a tornado. The aircraft can easily approach remote weather phenomena, but it has limited observation windows and resolution.

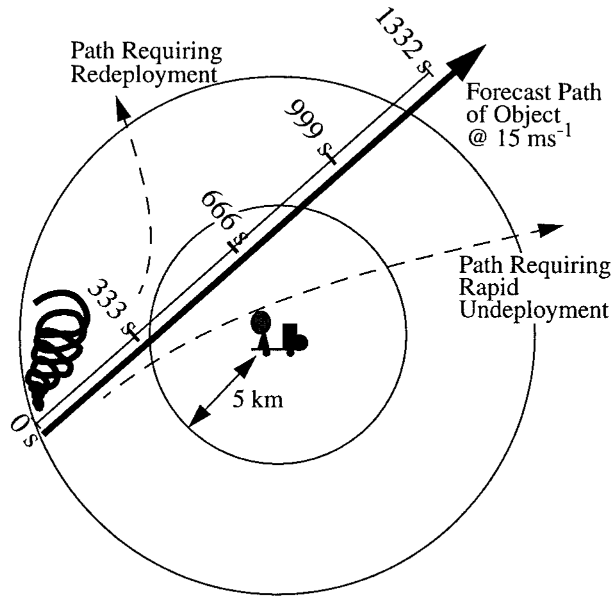

FIG. 3. Schematic of typical deployment scenario for a scanning mobile radar surveying a tornado. Several minutes of high-resolution, <100 m, data can be retrieved if the tornado closely follows the forecast path. Rapid undeployments and redeployments are necessary if the tornado deviates toward or away from the radar.

(Watson et al. 1996; Wakimoto et al. 1996). However, they have difficulty achieving extremely close ranges because of safety concerns, cannot use large antenna structures to achieve narrow beamwidths, and often follow flight paths that separate them from storms for 4–6-min periods (Fig. 2). For example, in the VORTEX-95 program, aircraft flew patterns that approached briefly within 12 km of tornadoes (Wakimoto et al. 1996). At a range of 12 km, the 2° beamwidth of the Electra Doppler Radar (ELDORA) antenna produces a beam that is 350 m in azimuthal extent, which is still too large to resolve finescale tornado structure (Rasmussen et al. 1994). Occasionally aircraft may be able to approach to within smaller ranges, but even then interbeam spacing caused by high aircraft velocities will limit resolution.

3. Ground-based mobile radars

A ground-based mobile radar system can travel to regions of interesting weather and approach to a range where finescale measurements are possible. The radar can remain stationary near the weather of interest or follow it if road conditions permit. Continuous finescale observations can be conducted for as long as the phenomenon remains within several kilometers of the radar. In a typical deployment where a mobile ground-based radar is positioned ahead of a system traveling at 15 m s^{-1}, continuous observations from a stationary deployment will likely be possible for roughly 1000 s (Fig. 3).

Bluestein et al. (1993) describe a mobile frequency modulation–continuous wave (FM–CW) radar system that has produced an estimate of the maximum velocity in a tornado vortex. However, the radar system is limited due to its broad beamwidth (5°, 262 m at 3 km) that prevents resolution of finescale structures in the tornado circulation. Low power reduces sensitivity and the lack of scanning capability effectively prevents three-dimensional mapping of weather phenomena. A mobile millimeter-wave radar system has been constructed and deployed (Bluestein et al. 1995). This radar has a 0.5° beamwidth and has produced high-resolution mappings of portions of a supercell thunderstorm. With larger antennas, millimeter-wave radar systems have the potential of measuring atmospheric features with scales of 10 m or even less. Millimeter-wave radars can collect data in environments where precipitation is light or absent, but they have a very limited ability to penetrate into heavy precipitation, which is often present in and around tornadoes (Lemon and Doswell 1979; Doswell and Burgess 1993). This complicates deployments since the radar must be located such that there is a relatively rain-free path between it and the phenomenon of interest. For studying storms in a rainy environment, a 3-cm radiation provided an optimal balance between resolution and rain penetration.

4. Doppler on Wheels

A prototype mobile Doppler radar that permits the study of rare, finescale, near-ground events, even in the

FIG. 4. The DOW scanning threatening weather during the VORTEX-95 field program. The 6′ dish and operator cabin are visible.

presence of significant precipitation, and that allows for the possibility of multiple-Doppler observations, has been constructed through a close collaboration among the University of Oklahoma (OU), the National Oceanic and Atmospheric Administration's National Severe Storms Laboratory (NSSL), and the National Science Foundation-sponsored National Center for Atmospheric Research (NCAR) and Center for the Analysis and Prediction of Storms (CAPS). This system, Doppler on Wheels (DOW), has characteristics similar to traditional stationary research weather radars, with the notable exceptions that it is fully mobile and employs an innovative PC-based digital IF data acquisition system. The radar has a narrow transmitted beam and full scanning capability, permitting the reconstruction of the three-dimensional structure of surveyed phenomena.

a. Mobile platform

The DOW (Figs. 4–6) is mounted on a modified medium-sized General Motors Chevrolet light duty panel truck (5.4-m length) provided by NSSL. Hydraulic outriggers allow for leveling and stability of the 4900-kg system. The maximum height of the antenna dish when pointed rearward for transport is 3.38 m (11′ 1″) above ground level (AGL) permitting travel on most roads and allowing easy loading onto cargo aircraft for rapid deployment to remote locations. When pointing vertically, the feedhorn extends to 3.68 m (12′ 1″) AGL, which is lower than most highway overpasses. Deployment costs are very low, mainly consisting of gasoline and operator salaries. The radar has scanned to collect data while mobile in headwinds of 40 m s^{-1}, and it is estimated that the vehicle can sustain winds and continue data collection in winds exceeding 50 m s^{-1}. A gasoline-fueled generator with a capacity of 9 kVA (208 V, three phase) provides power to all systems. The truck and generator proved to be somewhat underpowered. Future mobile radars, now in design, will use larger, more powerful vehicles and generators.

b. Transmitter

The DOW incorporates a surplus transmitter from the NCAR CP-2 radar (Keeler et al. 1989) that operates at 9.375 GHz. This transmitter has been modified to operate at a higher pulse repetition frequency (PRF), 2000 Hz, resulting in a Nyquist interval of 32 m s^{-1} (velocity folds at ±16 m s^{-1}, ±48 m s^{-1}, ±80 m s^{-1}), which is suitable, although not optimal, for tornado studies. The pulse length has been shortened to slightly less than 0.5 μs, both to reduce the duty cycle and to permit finer-scale range measurements (75 m). Peak power output is 45 kW. Use of this relatively high power transmitter enables the DOW to achieve sensitivities very similar to that of the pre-1994 CP-2 radar. The radar charac-

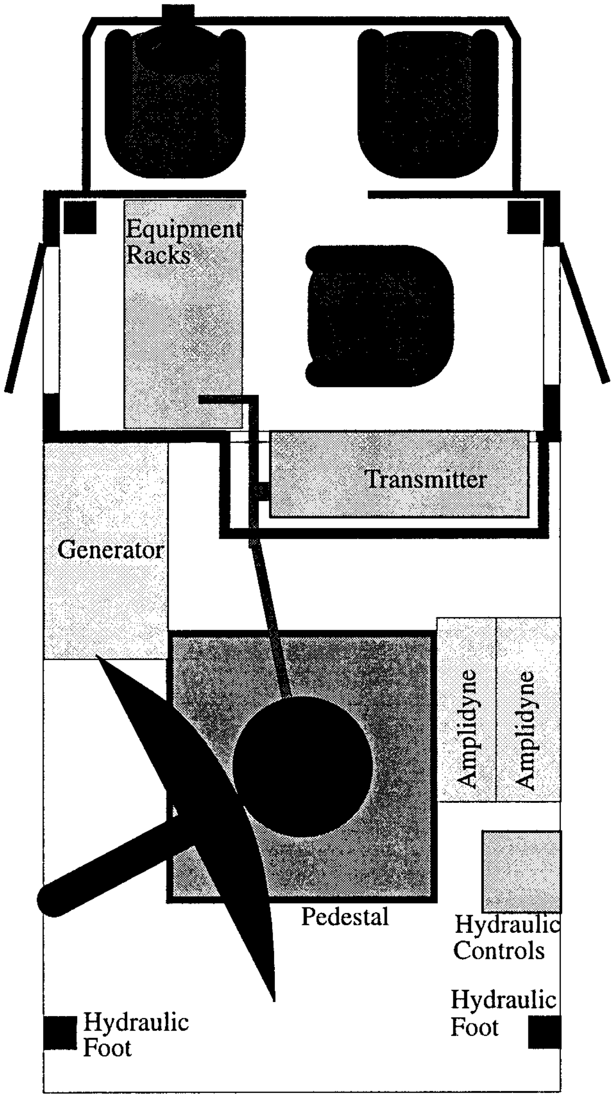

FIG. 5. Generalized layout of DOW mobile radar vehicle. Operator cabin holds transmitter, receiver, data acquisition, and antenna controller computers and hardware. Four hydraulic feet provide leveling and stabilization in high winds.

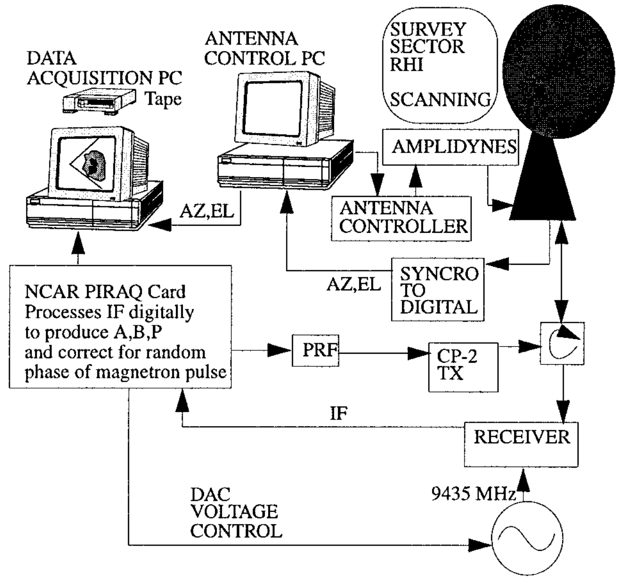

FIG. 6. Generalized schematic of the DOW system. Custom-built antenna controller provides flexible scanning patterns. Digital IF data acquisition in the PC processes signals to produce Doppler velocity, reflectivity, and other quantities that are archived on EXABYTE 8-mm tape.

teristics, similar in several categories to the NCAR CP-2 radar, are summarized in Table 1. The transmitter was of the noncoherent magnetron type, requiring software phase locking, accomplished digitally, in order to produce Doppler velocities. Future mobile systems, under construction, use higher power transmitters and higher frequency and staggered PRFs.

c. Antenna, pedestal, and scanning

A military surplus MP61 antenna with a diameter of 1.83 m (6′) was attached to a SCR-584 pedestal system (similar pedestals are used in the NCAR CP-3, CP-4, and ELDORA test bed radars), resulting in a beamwidth of 1.2°. Azimuth and elevation drive motors were capable of scanning up to 60° s^{-1} but were limited to 30° s^{-1} by the antenna controller. Since the first application of this radar was in severe weather, the rugged nature of this military pedestal system was desirable, despite the difficulties caused by its weight—estimated in excess of 1000 kg—and archaic design.

A 1.2° beamwidth provided beamwidths of 64 m at a range of 3 km. This, combined with the 500-ns pulse width described above, resulted in resolution volumes of 64 m × 64 m × 75 m, 310 000 m^3. This is less than 0.25% of that typically achievable with stationary radars and 4% that of airborne systems at typical ranges to tornadoes, thus providing a 25 to 400 times improvement in volumetric resolution. The narrow beamwidth and the ability to choose sites with good visibility permitted data to be retrieved to within 100 m of the ground in tornadoes.

The antenna controller for the DOW radar was implemented with a 486-class PC and a custom interface designed for utilization of the SCR-584 pedestal (Fig. 7). Antenna position is sensed by synchrotransducers that provide three phase signals to the interface. Two synchro-to-digital converters (SDCs) convert the three phase signals to weighted binary values. The binary values are converted to binary-coded decimal (BCD) using lookup tables for display. Binary position information is provided to the parallel input card in the PC.

The PC's internal 50-ms clock is used to sample the input antenna angular position values. The antenna angular position, antenna direction, and antenna rotation rate are calculated and sent to the data acquisition computer and the control program. Corrections are calcu-

TABLE 1. DOW radar characteristics.

Transmitter		
	Frequency	9.375 GHz
	Transmitter type	Magnetron
	Power	45 kW
	Pulse length	0.5 μs
	PRF	1000–2300 Hz (usually 2000 Hz)
	Unambiguous velocity range up to 37 m s^{-1} (usually 32 m s^{-1})	
Antenna		
	Diameter	1.83 m
	Beamwidth	1.2°
	Peak scanning rate	30° s^{-1} PPI or RHI (usually 10°–15° s^{-1})
	Polarization	H or V, not both
Receiver		
	Noise power	−110 dBm
	Minimum detectable signal at 3 km	−24 dBZ (0 dB SNR)
	Dynamic range	65 dB
Data acquisition		
	Data platform	486 or Pentium PC NCAR PIRAQ Digital IF
	Gates	285 without clutter filter 120 with 4-pole IIR clutter filter 120 with poly pulse pair
	Gate length	0.25–2.00 μs (37.5–300 m) (usually 75 m)
	Equivalent A/D bits	14
	Clutter suppression	15-dB 4-pole IIR
	Recording	EXABYTE 8-mm tape and disk
	Display	Real-time velocity, reflectivity, normalized coherent power, spectral width, power

lated with a predictive algorithm, and torque-limiting and antihunt features were implemented. Adjustments are output to the digital-to-analog converters (DAC) on the analog output card in the PC then to the isolation amplifiers in the interface. Analog drive circuits in the interface were designed to provide isolation, bias offset, and current drive for the field windings of the amplidynes. The original SCR-584 pedestal electronics system that was based on vacuum tube technology was not stable enough for this application.

Both PPI sector and RHI-type volume scans were possible providing scan capability comparable to typical research radars. PPI sector scans were configured to allow for volume update times of as little as 50 s. In the future, with the use of a planned additional DOW system, dual-Doppler retrievals at 50-s intervals will be possible.

A novel type of vertical wind profile can be obtained with the DOW. With the antenna pointed vertically, the truck can travel down a level highway and obtain traveling vertical wind profiles (Fig. 8). If the truck travels at 30 m s^{-1} and transmits with a PRF of 2000 Hz, pulses will be separated by only 15 mm, a small fraction of the beamwidth, maintaining pulse-to-pulse volume coherence. Radar beams can be integrated over many pulses, incorporating more independent samples without loss of resolution, in order to increase sensitivity. Using this method, two-dimensional slices through cold and warm frontal boundaries, gust fronts, microburst outflows, and other phenomena can be retrieved.

It is also possible to conduct pseudo-multiple-Doppler retrievals using an extension of the method employed by research aircraft (Hildebrand and Mueller 1985), by scanning quasi-steady-state phenomena first from one viewpoint, then traveling and scanning from other vantages separated by 30°–150° as shown in Fig. 9. If the

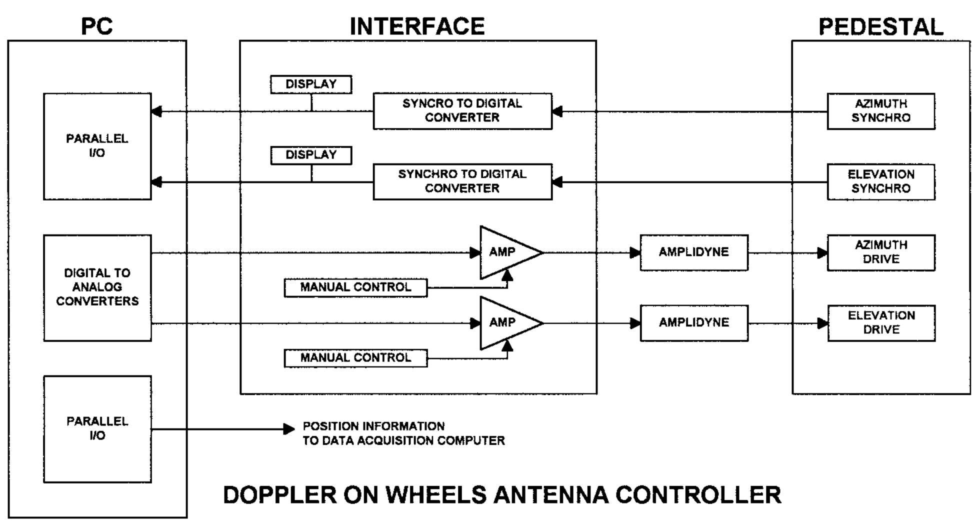

FIG. 7. Schematic of DOW antenna controller.

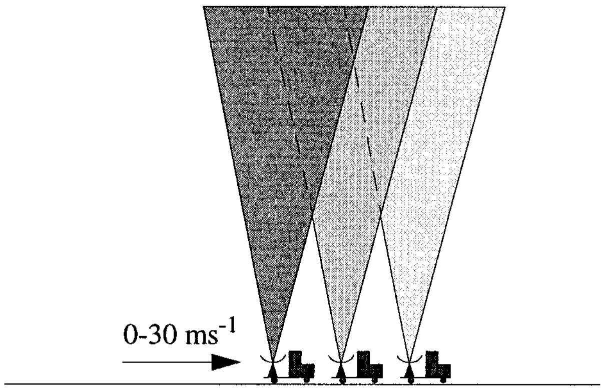

FIG. 8. Schematic illustration of traveling vertical wind profile conducted by DOW with antenna pointed vertically. Even at 30 m s^{-1}, there is significant pulse-to-pulse beam overlap resulting in coherent volumes for signal processing purposes.

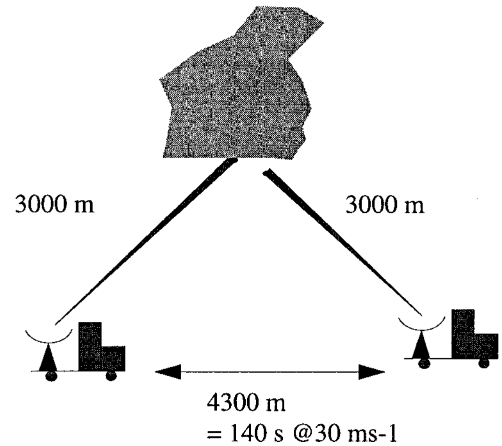

FIG. 9. Schematic illustration of pseudo-dual-Doppler technique conducted with DOW mobile radar. At short ranges, several kilometers or less, the time between observations from different vantages may be short enough to permit accurate and multiple-Doppler retrievals. Data may be collected continuously at intermediate locations, providing additional observations to overdetermine the solution.

range to a phenomena is approximately 3000 m, then the DOW would have to travel roughly 4300 m between perpendicular observations. At 30 m s^{-1}, this would require roughly 140 s, which is comparable to what is achieved with aircraft and suitable for many quasi-steady phenomena. Data may be collected continuously at intermediate locations in order to provide many observations from many vantage points, thus permitting highly overdetermined multiple-Doppler solutions to be calculated.

d. Receiver and data acquisition

The receiver design was typical for a research weather radar (Fig. 10) but used a local oscillator that was voltage controlled by software in the data acquisition system in order to track the varying frequency of the magnetron output. The receiver had approximately 60 dB of gain and a 65-dB dynamic range.

Data acquisition was accomplished on a PC-based card, the PIRAQ (PC Integrated Acquisition), developed at NCAR. The PIRAQ is a long format ISA bus card and is compatible with standard desktop PCs. This card, along with its PC host, compose a complete, inexpensive, high-performance radar data acquisition system. The system takes as input the radar IF signal and provides as output a multiparameter polar display (Doppler velocity, reflectivity, spectral width, normalized coherent power, or any calculated quantity), EXABYTE or CD-R tape data recording, magnetron AFC, and system timing.

The PIRAQ card [Fig. 11 (schematic)] provides several of the subsystems required for radar signal processing and control. A digital IF scheme (Randall 1991) is used to provide the I and Q baseband conversion. In this scheme, the 60-MHz IF input signal is downconverted to a second IF of 4 MHz that is sampled at 16 MHz with a resolution of 12 bits. These samples then pass through a pair of accumulators that implement two programmable decimating FIR filters, one each for I and Q matched to the typical rectangular radar pulse.

The digital IF scheme provides several advantages over its analog counterpart. Because it derives I and Q outputs digitally, it inherently provides phase and amplitude balance that are limited by the system noise floor. As a result, image rejection is typically greater than 60

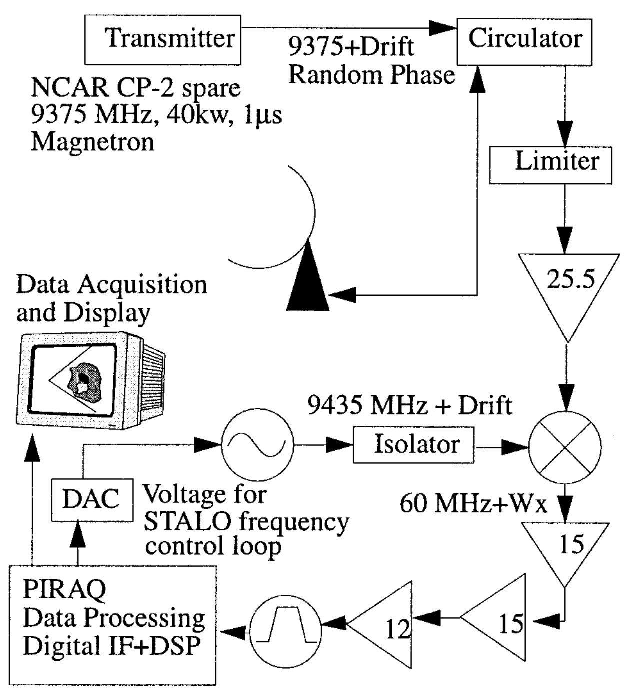

FIG. 10. Schematic of the DOW receiver. The data acquisition system provided a control voltage to the STALO so that its frequency tracked that of the drifting magnetron frequency.

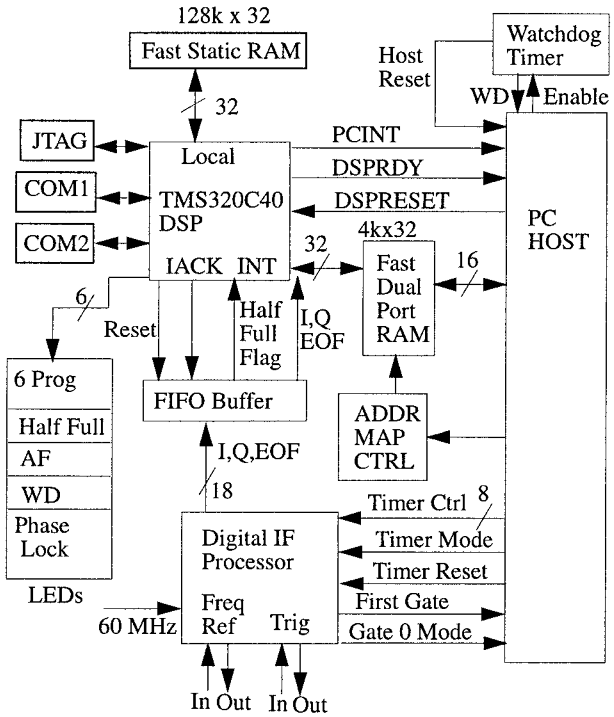

FIG. 11. Schematic of PIRAQ (PC-based digital IF Radar Acquisition) card.

dB. Another advantage is that DC drift and other low-frequency interference are essentially eliminated because of the characteristics of the digitally matched filter. In addition, the digital filter acts to reduce the quantization noise and thereby increases the system dynamic range. For the case where the filter is programmed to match a 1-μs pulse, this can result in a 10-dB increase to 70 dB of dynamic range.

The PIRAQ card contains a flexible timing generator. The timer sets the number of range gates to be sampled and the range gate spacing. There are three possible trigger modes: internal trigger, external trigger, and external sync. The internal trigger mode allows the PIRAQ to generate its own PRF, which is then available as an output to control external devices. The external trigger mode slaves the PIRAQ to an external PRF via an external trigger input connector. A variable delay can be programmed in this mode to offset the start of timing with respect to the external trigger. The external sync mode can be used to synchronize the internal triggers to an external event. All of these settings are programmed through I/O ports on the ISA bus. In all of these modes, the timing is referenced to an oscillator that can be phase locked to an external master oscillator. [This is particularly useful in bistatic multiple-Doppler applications; Wurman (1994).] In the DOW system, the external trigger mode is used to lock to a special ISA bus timing generator card that is capable of generating staggered pulse timing. There is a special mode of the timing generator that is used for magnetron radars. In this mode the raw analog/digital (A/D) samples from the first gate are latched into the FIFO (first in, first out) along with the normal I and Q data. When the first gate is aligned in time with the transmit pulse, these raw A/D samples can be used to implement a digital discriminator to be used as the error signal in an AFC loop (Li et al. 1994; Nutten et al. 1979).

Digital I's and Q's are fed into a FIFO register on the PIRAQ card. The FIFO's half-full flag is used to interrupt the onboard TMS320C40 digital signal processor chip operating at 50 MHz. The DSP chip has 128 000 words of memory on its local bus and 16 000 words of true dual-port memory on its global bus. The other side of the dual-port memory is mapped into the ISA bus memory space of the PC host and used as program and transfer data by the system.

The DOW data acquisition system uses a PIRAQ, a PRF generator, and a digital/analog (D/A) card to perform all the functions necessary to retrieve Doppler from its magnetron transmitter. The PRF generator card creates the base PRF. This card can generate a staggered pulse repetition time (PRT) for a planned upgrade. The output pulse triggers the transmitter and the PIRAQ card. The PIRAQ delay is adjusted so that the first gate samples the transmit pulse so its phase can be determined. The receiver is specifically designed such that when it saturates it does not overload the PIRAQ front end. Also, the 16-MHz raw samples are used to adjust the D/A card voltage output. This voltage steers the receiver X-band local oscillator to maintain an approximately 60-MHz IF center frequency. Each I and Q is normalized with the phase offset as measured from the transmit pulse. This results in a set of pseudo-coherent I's and Q's from which Doppler data can be retrieved. The PIRAQ DSP performs an optional clutter filter algorithm, the digital discriminator algorithm, and the standard pulse-pair algorithm. The first and second moments are generated and the results placed in the dual-port memory. In addition, a flag is set in dual-port memory. The PC host recognizes this flag and further processes the moments to arrive at the final products: velocity, power, spectral width, normalized coherent power, reflectivity, and coherent reflectivity. The PC uses a lookup-table-based display algorithm to efficiently display each parameter in standard PPI or RHI format. The PC records the pulse pair moments to either disk, CD-R or EXABYTE tape, in real time. During the 1995 deployment, the system was capable of processing approximately 33 beams per second with 285 gates per beam (approximately one-half of this when using a clutter filter). Data acquisition was limited to roughly 20 beams per second by the rate at which the PC could display and archive data. The incorporation of PCs using Pentium 133-MHz chips has eliminated this constraint. Sampling rates can be adjusted in the range of 0.25–10 μs in 0.25-μs steps. The complete time series of I's and Q's was collected at one adjustable range. PC resident software allows adjustments during operations of most

DSP parameters, including clutter filtering, gate length, integration time, and full spectrum sampling range, with almost no loss of data.

5. First deployments and sample results

High spatial and temporal resolution data were collected in a wide variety of weather phenomena, including several tornadoes, during the DOW's first deployment season during VORTEX. These data are being analyzed and early results are presented elsewhere (Wurman et al. 1996a, Wurman et al. 1996b; Straka et al. 1996). Representative data from a tornadogenesis event that occurred near Rolla, Kansas, illustrate the capabilities of the DOW (Fig. 12). For the first time, high-resolution detail is revealed in the hook echo and the coil-like signature of the nascent tornado. A moderately intense velocity couplet associated with the parent circulation is visible. A tornado formed approximately 50–100 s after this data were taken. The DOW has been deployed in the Small Cumulus Microscale Study and the FLATLAND experiment in 1996. During a VORTEX operational period several small-scale circulations associated with dust devils were detected in Texas. Data from one of these events are shown in Fig. 13. Multiple small velocity couplets are revealed along a low reflectivity convergence line. More recently, the DOW revealed high amplitude, 600-m scale, boundary layer rolls during the landfall of Hurricane Fran (September 1996).

6. Summary and future plans

A mobile weather research radar, with capabilities typical of stationary research radars, can be employed to successfully collect data in tornadoes and other weather phenomena. This type of radar can collect data at very fine temporal and spatial resolution, helping to answer many questions concerning the physics of these phenomena. The digital IF scheme and pseudocoherent processing executed on the NCAR PIRAQ card have also proved successful, demonstrating that this low-cost solution is practical.

Continued studies using the DOW are planned and the system is continually being upgraded. Staggered PRT capability in order to increase the Nyquist interval is under development. A larger antenna (2.44 m, 0.9°) has been added to enhance resolution (40 m at 3 km), and dual 250-kW transmitters capable of dual-frequency 0.1–2.0-μs pulses at up to 9 kHz are planned.

A second mobile radar, DOW2, has recently been developed. It incorporates improved features drawing on the experience gained from the development and operation of the first system. These two mobile radars will allow mobile dual-Doppler studies of tornadoes and many other phenomena. This new system employs a 250-kW transmitter with pulses of 0.2–1.0-μs duration at up to 5 kHz and staggered PRFs. In combination with a 2.44-m (0.9°) antenna, this will permit 40 m $\times$ 40 m $\times$ 40 m resolution data to be retrieved at 3-km ranges. The possibility of incorporating a phased array antenna that will permit rapid-scan dual-Doppler, remote, possibly mobile bistatic receivers (Wurman 1994) that permit mobile multiple-Doppler synthesis are being explored as are modifications to incorporate dual-polarization and additional shorter and longer wavelengths.

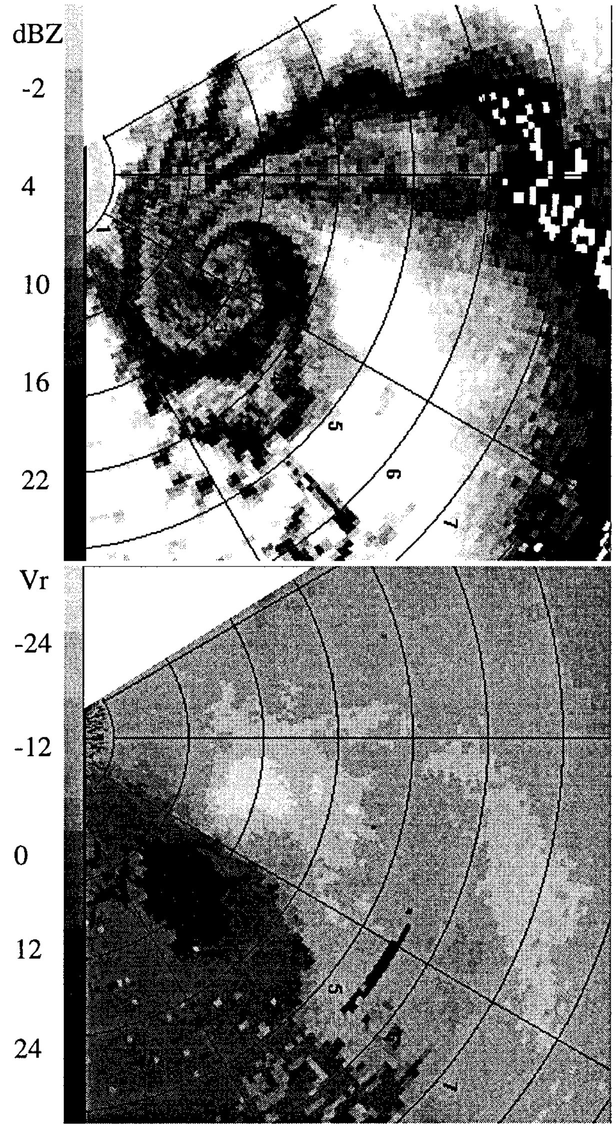

FIG. 12. Reflectivity (top) and radial velocity (bottom) fields during tornadogenesis near Rolla, Kansas, at 2250:14 UTC 1 June 1996. The data are from a ground-level scan. Range rings are at 1-km intervals with the center of the storm 2.5 km from DOW, which is off the left of the plotted area. Resolution volumes are 40 m $\times$ 40 m $\times$ 75 m at the tornado center. The hook echo associated with the tornado protrudes from the supercell storm to the right of the plot area. The coiled feature at the tip of the hook is indicative of an incipient tornado. A velocity couplet of approximately $\pm$30 m s^{-1} over 800 m is present; 240 s later, the scale of the couplet had decreased to 400 m in the mature tornado. Reflectivity levels are too low due to a radar malfunction.

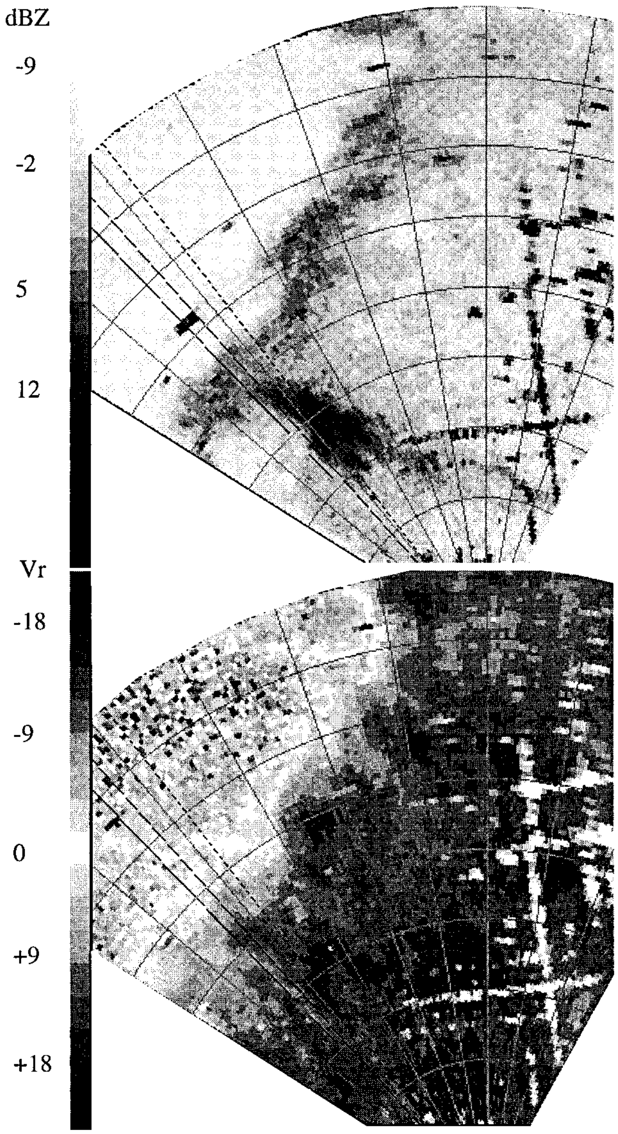

FIG. 13. Reflectivity (top) and radial velocity (bottom) fields in Texas convergence line recently containing dust devils 2018:33 UTC 3 June 1995. The data are from 2.0° elevation scan. Range rings are at 2-km intervals. The higher reflectivity convergence line is clearly visible. Two velocity couplets suggestive of rotation are visible at 10- and 15-km range. Dust devils had been visually observed along this line several minutes before these radar observations. Linear features are ground clutter caused by power lines.

In particular, 8-mm signals could be transmitted simultaneously through the existing antennas to provide a 0.2″ beamwidth and 10-m resolution at 3-km range.

REFERENCES

Bluestein, H. B., and J. H. Golden, 1993: A review of tornado observations. *The Tornado: Its Structure, Dynamics, Prediction and Hazards, Geophys. Monogr.,* No. 79, Amer. Geophys. Union, 19–39.

——, J. G. LaDue, H. Stein, D. Speheger, and W. P. Unruh, 1993: Doppler radar wind spectra of supercell tornadoes. *Mon. Wea. Rev.,* **121,** 2200–2221.

——, A. L. Pazmany, J. C. Galloway, and R. E. McIntosh, 1995: Studies of the substructure of severe convective storms using a mobile 3-mm wavelength Doppler radar. *Bull. Amer. Meteor. Soc.,* **76,** 2155–2169.

Brandes, E. A., 1993: Tornadic thunderstorms characteristics determined with Doppler radar. *The Tornado: Its Structure, Dynamics, Prediction and Hazards, Geophys. Monogr.,* No. 79, Amer. Geophys. Union, 143–160.

Burgess, D. W., R. J. Donaldson, and P. R. Desrochers, 1993: A review of tornado observations. *The Tornado: Its Structure, Dynamics, Prediction and Hazards, Geophys. Monogr.,* No. 79, Amer. Geophys. Union, 203–222.

Doswell, C. A., III, and D. W. Burgess, 1993: Tornadoes and tornadic storms: A review of conceptual models. *The Tornado: Its Structure, Dynamics, Prediction and Hazards. Geophys. Monogr.,* No. 79, Amer. Geophys. Union, 161–172.

Doviak, R. J., and D. S. Zrnic, 1993: *Doppler Radar and Weather Observations.* Academic Press, 562 pp.

Fujita, T. T., 1978: Manual of downburst identification for project NIMROD. University of Chicago SMRP Research Paper 156, 104 pp. [NTIS PB 286048.]

Harris, F. I., and J. C. Fankhauser, 1978: A complex convective storm system studied by multiple Doppler radar analysis. Preprints, *18th Conf. on Radar Meteorology,* Atlanta, GA, Amer. Meteor. Soc., 207–211.

Hildebrand, P. H., and C. K. Mueller, 1985: Evaluation of meteorological airborne Doppler radar. Part I: Dual-Doppler analyses of air motions. *J. Atmos. Oceanic Technol.,* **2,** 362–380.

Kaplan, J., and M. DeMaria, 1995: A simple emperical model for predicting the decay of tropical cyclone winds after landfall. *J. Appl. Meteor.,* **34,** 2499–2512.

Keeler, J. R., B. W. Lewis, and G. R. Gray, 1989: Description of NCAR/FOF CP-2 meteorological Doppler radar. Preprints, *24th Conf. on Radar Meteorology,* Tallahassee, FL, Amer. Meteor. Soc., 589–592.

Knight, C. A., and L. J. Miller, 1993: First radar echoes from cumulus clouds. *Bull. Amer. Meteor. Soc.,* **74,** 179–188.

Lemon, L. R., and C. A. Doswell III, 1979: Severe thunderstorm evolution and mesocyclone structure as related to tornadogenesis. *Mon. Wea. Rev.,* **107,** 1184–1197.

Lhermitte, R., and E. Williams, 1985: Thunderstorm electrification: A case study. *J. Geophys. Res.,* **90,** 6071–6078

Li, H., A. J. Illingworth, and J. Eastment, 1994: A simple method of Dopplerizing a pulsed magnetron radar. *Microwave J.,* **37** (4), 226–235.

Miller, L. J., 1978: Horizontal airflow and precipitation fallspeed in a convective system from triple Doppler radar measurements. Preprints, *18th Conf. on Radar Meteorology,* Atlanta, GA, Amer. Meteor. Soc., 207–211.

Nutten, B., P. Amayenc, M. Chong, D. Hauser, F. Roux, and J. Testud, 1979: The RONSARD Radars: A Versatile C-Band Dual Doppler Facility. *IEEE Trans. Geosci. Electron.,* **GE 174,** 281–288.

Randall, M., 1991: A digital IF scheme for processing radar data. Preprints, *25th Int. Conf. on Radar Meteorology,* Paris, France, Amer. Meteor. Soc., 821–919.

Rasmussen, E. N., J. M. Straka, R. P. Davies-Jones, C. E. Doswell III, F. Carr, M. Eilts, and D. R. MacGorman, 1994: Verification of the origins of rotation in tornadoes experiment: VORTEX. *Bull. Amer. Meteor. Soc.,* **75,** 995–1006.

Ray, P. S., K. K. Wagner, K. W. Johnson, J. J. Stephens, W. C. Bumgarner, and E. A. Mueller, 1978: Triple-Doppler observations of a convective storm. *J. Appl. Meteor.,* **17,** 1201–1212.

Raymond, D. J., and A. M. Blythe, 1989: Precipitation development in a New Mexico thunderstorm. *Quart. J. Roy. Meteor. Soc.,* **115,** 1397–1423.

Schwiesow, R. L., 1981: Horizontal velocity structure in waterspouts. *J. Appl. Meteor.,* **20,** 349–360.

Snow, J. T., and T. M. McClelland, 1990: Dust devils at White Sands

Missile Range, New Mexico: Temporal and spatial distributions. *J. Geophys. Res.,* **95,** 13 707–13 721.

Straka, J. M., J. Wurman, and E. N. Rasmussen, 1996: Observations of the low-levels of tornadic storms using a portable X-band Doppler radar. Preprints, *18th Conf. on Severe Local Storms,* San Francisco, CA, Amer. Meteor. Soc., 11–16.

Wakimoto, R. M., and V. N. Bringi, 1988: Dual-polarization observations of microbursts associated with intense convection: The 20 July storm during the MIST project. *Mon. Wea. Rev.,* **116**, 1521–1539.

——, and J. W. Wilson, 1989: Non-supercell tornadoes. *Mon. Wea. Rev.,* **117,** 1113–1140.

——, and B. E. Martiner, 1992: Observations of a Colorado Tornado. Part II: Combined photogrammetric and Doppler radar analysis. *Mon. Wea. Rev.,* **120,** 522–533.

——, and P. G. Black, 1994: Damage survey of Hurricane Andrew and its relationship to the eyewall. *Bull. Amer. Meteor. Soc.,* **75,** 189–200.

——, W. C. Lee, H. B. Bluestein, C.-H. Liu, and P. H. Hildebrand, 1996: ELDORA observations during VORTEX 95. *Bull. Amer. Meteor. Soc.,* **77,** 1465–1481.

Wilson, J. W., 1986: Tornadogenesis by nonprecipitating-induced shearlines. *Mon. Wea. Rev.,* **114,** 270–284.

Wurman, J., 1991: Forcing mechanisms of thunderstorm downdrafts. Sc.D. thesis, Massachussets Institute of Technology, 387 pp. [Available from Massachusetts Institute of Technology, 77 Massachusetts Avenue, Cambridge, MA 02142.]

——, 1994: Vector winds from a bistatic multiple-Doppler network. *Bull. Amer. Meteor. Soc.,* **75,** 983–994.

——, J. M. Straka, and E. N. Rasmussen, 1996a: Preliminary radar observations of the structure of tornadoes. Preprints, *18th Conf. on Severe Local Storms,* San Francisco, CA, Amer. Meteor. Soc. 17–22.

——, ——, and ——, 1996b: Fine-scale Doppler radar observations of tornadoes. *Science,* **272,** 1774–1777.

Zrnic, D. S., D. W. Burgess, and L. Hennington, 1985: Doppler spectra and estimated windspeed of a violent tornado. *J. Climate Appl. Meteor.,* **24,** 1068–1081.